Universal transport properties of asymmetric chiral quantum dots

A. F. Macedo-Junior and A. M. S. Macêdo
Departamento de Física, Laboratório de Física Teórica e Computacional, Universidade Federal de Pernambuco, Recife, 50670-901 Pernambuco, Brazil

(Received 19 December 2007; revised manuscript received 7 March 2008; published 9 April 2008)

We study the transport properties of a quantum dot with sublattice symmetry (chiral symmetry) coupled to two electron reservoirs via asymmetric ideal point contacts. The joint distribution of transmission eigenvalues is obtained from a maximum-entropy principle, and we calculate all moments and the full distribution of conductance for some cases of physical interest in the extreme quantum limit of few open channels. A Brownian motion model is used to obtain the average conductance for an arbitrary number of open channels in each lead. All analytical results are confirmed by numerical implementations of the Mahaux–Weidenmüller formula for the scattering matrix.

DOI: 10.1103/PhysRevB.77.165313 PACS number(s): 73.23.−b, 05.40.−a

I. INTRODUCTION

In the absence of the Coulomb interaction, the electron dynamics in phase coherent conductors can be well described via the Landauer–Büttiker scattering formalism.[1] In this approach, transport observables such as conductance, shot-noise power, or higher cumulants of the charge-counting statistics[2] are directly related to the scattering (S) matrix of the system. Universal statistical properties of such observables can be obtained by means of a random-matrix theory (RMT) formulation of the transport problem. There are two such approaches:[3] the Hamiltonian and the scattering matrix technique (which includes transfer matrices). In the first one, the Hamiltonian of the system is modeled by a Hermitian random matrix, and the associated S-matrix is obtained through quantum scattering theory. In the second case, the RMT is directly constructed for the S-matrix by means of a maximum-entropy principle, which is global, i.e., involves the scattering properties of the whole system, in the case of ballistic chaotic cavities and local, i.e., only single scattering from a thin slice is considered, for the transfer matrix description of disordered wires. For chaotic quantum dots, strong arguments in favor of the equivalence of these two approaches have been presented in Refs. 4–6.

The fundamental feature of the maximum-entropy technique is the possibility to directly address the universal stochastic properties of the S-matrix bypassing the need to specify irrelevant microscopic details of the underlying Hamiltonian. The only relevant information concerns the basic intrinsic symmetries of the Hamiltonian, such as time reversal (TR), spin rotation (SR), particle hole, and chiral. There are ten universality classes which directly follow from a one-to-one correspondence[7] with Cartan's table of symmetric spaces.[8] These ten symmetry classes can be further divided into three categories: Wigner–Dyson, chiral, and Bogoliubov–de Gennes (BdG). The Wigner–Dyson class was the first thoroughly studied and contains the three standard ensembles of classical RMT.[20] It is appropriate to describe transport on conventional disordered conductors and ballistic chaotic cavities. The chiral class applies to systems with off-diagonal disorder and the BdG class is used in the description of quasiparticles in weakly disordered unconventional superconductors.

During the last decade, the proof of the mathematical existence and the physical realization of new universality classes resulted in an outburst of activity in this field. Some of the addressed problems concerned the effects of the novel symmetries on physical properties of previously studied systems. In this line of research, transport properties of systems, such as quantum wires and quantum dots with chiral symmetry, have attracted much attention. The chiral symmetry naturally emerges on systems in which the disorder is completely off diagonal, such as in the random hopping model.[9,10] The nearest-neighbor random hopping connecting sites of different sublattices in a bipartite topology implies an additional discrete symmetry, in which the single particle energy changes sign under a transformation that changes the sign of the wave function in one sublattice, but not in the other. As a consequence, the spectrum is symmetric about the energy $\varepsilon=0$ and, at this special point, the system shows very unusual spectral and transport properties, which are signatures of the chiral symmetry class.

Quasi-one-dimensional disordered conductors with chiral symmetry (chiral quantum wires) have been intensively studied, both analytically and numerically, with the aid of the random-transfer-matrix approach.[9–14] This disordered system has a bipartite structure with a random hopping connecting sites in different sublattices and is coupled via ideal leads, also a bipartite lattice, to two electron reservoirs. Some of the remarkable results reported in these works include the anomalous behavior of the density of states near the band center and the dependence of the localization length on the parity of the number of open channels. Similar results were obtained from an alternative approach based on the nonlinear σ model.[15,16] In addition, these works reported a different parity effect which depends on the total number of sites in the chiral quantum dot and affects both its spectral and transport properties.

A chiral quantum dot can be defined as the zero-dimensional limit of a quantum wire with sublattice symmetry. A systematic study of transport properties of a two-terminal chiral quantum dot was presented in Ref. 18 in a model that corresponds to the zero-dimensional limit of that introduced in Ref. 10. It is assumed that there is a finite density of zero-energy eigenstates responsible for transport at the chiral point.[17] It is also assumed that the coupling of the system to the leads is ideal (no barriers), symmetric, i.e., the same number of open scattering channels in both leads ($N_1 = N_2$), and involves sites of both sublattices, which allows for the existence of a nonvanishing electric current through the system.[16] Based on a maximum-entropy S-matrix ensemble, the authors showed that the presence of chiral symmetry dramatically affects transport observables in the limit of few propagation modes, but in the semiclassical limit, the chiral symmetry affects only the quantum correction terms, which are more sensitive to phase coherence. Transport and spectral properties of a chiral quantum dot were recently studied in a different context in Ref. 19, which considers chiral dots with absorption coupled to an electron reservoir via a single-channel lead.

In this work, we generalize the analysis based on the maximum-entropy S-matrix approach presented in Ref. 18 to the case of asymmetric ideal contacts, i.e., by allowing for different numbers of propagation modes in each lead. We also show some calculational details not included in Ref. 18 and derive additional results. Furthermore, we formulate the problem in terms of the Hamiltonian approach and show that the compatibility between the chiral constraint on the Hamiltonian and on the S-matrix is guaranteed if we impose an additional constraint on the coupling matrix. The analytical results obtained from the maximum-entropy S-matrix ensemble are compared to numerical ones obtained from the Hamiltonian approach, yielding perfect agreement.

The paper is organized as follows. In Sec. II, we briefly review the scattering approach, list the basic symmetry constraints imposed on the S-matrix, and write the observables of interest in terms of transmission eigenvalues. Next, we present the two random-matrix approaches to the problem. In Sec. II A, we construct the maximum-entropy S-matrix ensemble and obtain the joint transmission eigenvalue distribution. In Sec. II B, we introduce the chiral random Hamiltonian of the closed dot and relate it to the S-matrix of the open dot through the Mahaux–Weidenmüller formula. In Sec. III, we obtain analytical expressions for the average conductance and shot-noise power and their full distributions in the limit of few open channels. We also compare the analytical formulas with numerical results.

II. SCATTERING FORMALISM

Our model system is a two probe setup consisting of a chiral quantum dot, coupled to two electrical reservoirs by semi-infinite ideal leads, with N_1 and N_2 open propagation channels. We shall consider the general asymmetric case assuming, without loss of generality, that $N_2 > N_1$ and defining $m = N_2 - N_1$ and $N = \min(N_1, N_2)$.

In the leads, we have incoming and outgoing plane wave states described, respectively, by N_i-dimensional vectors I_i and O_i, $i = 1,2$. By definition, the scattering matrix S relates these amplitudes through

$$\begin{pmatrix} O_1 \\ O_2 \end{pmatrix} = S \begin{pmatrix} I_1 \\ I_2 \end{pmatrix}. \tag{1}$$

It is conveniently written in the following block structure:

$$S = \begin{pmatrix} s^{11} & s^{12} \\ s^{21} & s^{22} \end{pmatrix} = \begin{pmatrix} r & t' \\ t & r' \end{pmatrix}, \tag{2}$$

in which the blocks r and r' denote reflection matrices, while t and t' are transmission matrices. Each block s^{ij} is an $N_i \times N_j$ matrix.

Flux conservation implies that the S-matrix must be unitary,

$$S^{\dagger} S = 1. \tag{3}$$

Sublattice symmetry, represented by the invariance of the scattering properties of the system under a transformation that interchanges incoming and outgoing waves, changing the sign of their energy, leads to the constraint[10] $S^{\dagger}_{-\varepsilon} = S_{\varepsilon}$. Since we are interested in describing transport properties at the chiral point $\varepsilon = 0$, the scattering matrix becomes Hermitian,

$$S^{\dagger} = S. \tag{4}$$

In the absence of other symmetries, the S-matrix of the chiral ensemble must satisfy the above requirements only. This specifies the chiral-unitary class, characterized by Dyson's index $\beta = 2$. Invariance of the physical system under TR and SR imposes additional constraints on the scattering matrix. For systems with TR and RS symmetries, the S-matrix must be symmetric,

$$S^{T} = S. \tag{5}$$

Conditions (3)–(5) define the chiral-orthogonal class, characterized by $\beta = 1$. On the other hand, for systems with TR but without SR symmetries there is an additional spin degree of freedom for each scattering state, yielding a factor 2 in the order of the scattering matrix. Therefore, S becomes a $2(N_1 + N_2) \times 2(N_1 + N_2)$ matrix, which can be conveniently represented as an $(N_1 + N_2) \times (N_1 + N_2)$ quaternion matrix. For such system, S must be a self-dual quaternion matrix,[20]

$$\bar{S} = S. \tag{6}$$

Conditions (3), (4), and (6) define the chiral-symplectic class, characterized by $\beta = 4$.

The unitarity of the S-matrix implies that the N_2-order matrix $tt^{\dagger}$ has the same eigenvalues as the N_1-order matrix $t' t'^{\dagger}$, plus a set of $m = N_2 - N_1$ zero eigenvalues. The nonzero eigenvalues τ_i, $(i = 1, \ldots, N_1)$ are called the transmission eigenvalues of the system. Transport properties can be related to the transmission eigenvalues by means of the Landauer–Büttiker scattering theory. We write below, as instances, the dimensionless conductance and shot-noise power in terms of the transmission matrix,

$$g = \mathrm{Tr}\, tt^{\dagger} = \sum_{i=1}^{N_1} \tau_i, \tag{7}$$

$$p = \mathrm{Tr}[tt^{\dagger}(1 - tt^{\dagger})] = \sum_{i=1}^{N_1} \tau_i (1 - \tau_i). \tag{8}$$

In the following section, we discuss the two RMT approaches to obtain the scattering matrix distribution of a chiral quantum dot.

A. S-matrix ensemble: Maximum-entropy approach

The statistical characteristics of transport observables can be obtained by averaging over an ensemble of scattering matrices. We may therefore introduce the probability to find a system with scattering matrix in a neighborhood dS of some given S by

$$dP_\beta(S) = \mathcal{W}_\beta(S) d\mu^{(\beta)}(S), \tag{9}$$

where $d\mu^{(\beta)}(S)$ is the, β-dependent, invariant Haar's measure of the appropriate symmetry group. The S-matrix ensemble can be constructed by maximizing the Shannon information entropy,[21]

$$\mathcal{S} = -\int d\mu^{(\beta)}(S)\mathcal{W}_\beta(S)\ln \mathcal{W}_\beta(S), \tag{10}$$

subject to the symmetry constraints of S and normalization of $\mathcal{W}_\beta(S)$, yielding $\mathcal{W}_\beta(S)=\text{const}$. This result means that the scattering matrix is uniformly distributed over the unitary group and that the differential probability is completely defined by the corresponding Haar's measure,

$$dP_\beta(S) \propto d\mu^{(\beta)}(S). \tag{11}$$

Such an approach has the advantage of directly accessing the universal distribution of the scattering matrix, without the need to build a detailed microscopic Hamiltonian.

Following Ref. 22, we represent the chiral S-matrix in the polar parametrization,

$$S = \begin{pmatrix} u & 0 \\ 0 & v \end{pmatrix} \begin{pmatrix} -\cos 2\Phi & 0 & \sin 2\Phi \\ 0 & \mathbb{1}_m & 0 \\ \sin 2\Phi & 0 & \cos 2\Phi \end{pmatrix} \begin{pmatrix} u^{-1} & 0 \\ 0 & u^{-1} \end{pmatrix}, \tag{12}$$

where u and v are $N_1 \times N_1$ and $N_2 \times N_2$ matrices, both orthogonal, unitary, and real self-dual quaternion for $\beta=1$, 2, and 4, respectively, and $\mathbb{1}_m$ is the m-dimensional unit matrix. The matrix Φ is diagonal and contains N_1 nonvanishing eigenvalues $0 \le \phi_i \le \pi/2$, related to the transmission eigenvalues by $\tau_i=\sin^2(2\phi_i)$. Note that in the case $N_1=N_2$ $(m=0)$, this representation reduces to that used in Ref. 18. In such a parametrization, the dimensionless conductance and shot-noise power are, respectively, given by

$$g = \sum_i \sin^2(2\phi_i), \tag{13}$$

$$p = \sum_i \sin^2(2\phi_i)\cos^2(2\phi_i). \tag{14}$$

The invariant measure is calculated in Appendix A for all symmetry classes. Upon integrating over the angular part, we arrive at the reduced distribution,

$$P(\{\phi\}) \propto \prod_{i<j} \prod_{\sigma=\pm} |\sin(\phi_i + \sigma\phi_j)|^\beta \prod_{i=1}^{N_1} \sin^{\beta-1}(2\phi_i)\sin^{\beta m}(\phi_i). \tag{15}$$

In the particular case of symmetric contacts $(m=0)$, this expression reduces to that presented, without derivation, in Ref. 18. In this case, it was possible to connect the chiral S-matrix ensembles to Cartan's table of symmetric spaces. In the general case $(m \neq 0)$, however, such a directed connection is not possible. Nevertheless, the non-Cartan parametrization, recently discussed by Caselle and Magnea,[23] could be used to obtain Eq. (15). For conventional quantum dots with asymmetric contacts, the joint distribution of transmission eigenvalues was first stated, without proof, in Ref. 3. A deduction was recently put forward in Ref. 24.

B. Hamiltonian approach

Systems with chiral symmetry are described by Hamiltonians with the following off-diagonal block structure,

$$\mathcal{H} = \begin{pmatrix} 0 & H \\ H^\dagger & 0 \end{pmatrix}, \tag{16}$$

in which the block H is a rectangular matrix with L_1 rows and L_2 columns, so that the order of $\mathcal{H}$ is $M=L_1+L_2$. We assume that $L_1 > L_2$, in which case the matrix $\mathcal{H}$ has exactly $N_z=L_1-L_2$ zero eigenvalues, whose corresponding eigenfunctions are denoted as zero modes. The remaining $M-N_z$ eigenvalues occur in symmetrical pairs $\pm\varepsilon_k$, where ε_k denotes the positive square roots of the eigenvalues of $H^\dagger H$.[25] Chiral Hamiltonian (16) satisfies the following constraint,

$$\Sigma_z \mathcal{H} \Sigma_z = -\mathcal{H}, \quad \Sigma_z = \begin{pmatrix} \mathbb{1}_{L_1} & 0_{L_1 \times L_2} \\ 0_{L_2 \times L_1} & -\mathbb{1}_{L_2} \end{pmatrix}, \tag{17}$$

which is a generalization of the Pauli matrix σ_z.

We assume that, in the universal regime, the block H can be chosen as a member from the chiral Gaussian ensemble. The probability distribution is given by

$$P(H) \propto e^{-2\beta M \,\mathrm{Tr}\, H^\dagger H}. \tag{18}$$

Such ensembles have been used in the study of spectral properties of the QCD Dirac operator.[26]

The scattering matrix of an open system is obtained from the Hamiltonian $\mathcal{H}$ of the corresponding closed system by means of the Mahaux–Weidenmüller formula,[27]

$$S(E) = 1 - 2\pi i W^\dagger \frac{1}{E - \mathcal{H} + i\pi WW^\dagger} W, \tag{19}$$

in which W is an $M \times (N_1+N_2)$ nonrandom matrix describing the coupling of the resonance states in cavity to the propagating states in the guides. For our two-terminal problem, it has the following structure:[28]

$$W_{\mu,n} = \begin{cases} (W_1)_{\mu,n}, & n = 1, \ldots, N_1 \\ (W_2)_{\mu,n-N_1}, & n = N_1+1, \ldots, N_1+N_2. \end{cases} \tag{20}$$

The matrices W_j, $j=1,2$, describe the coupling to each of the two guides. By explicitly using these matrices, we can write the S-matrix in the familiar block structure [Eq. (2)] with transmission and reflection matrices given by

$$r = 1 - 2i\pi W_1^\dagger D^{-1} W_1, \tag{21}$$

$$t' = - 2i\pi W_1^\dagger D^{-1} W_2, \tag{22}$$

$$t = - 2i\pi W_2^\dagger D^{-1} W_1, \tag{23}$$

$$r' = 1 - 2i\pi W_2^\dagger D^{-1} W_2, \tag{24}$$

where

$$D = E - \mathcal{H} + i\pi(W_1 W_1^\dagger + W_2 W_2^\dagger). \tag{25}$$

Note that Eqs. (21)–(24) give the full S-matrix, although we only need the transmission matrix [Eq. (23)] to calculate the observables of interest. The universality of the results, and the agreement with the maximum-entropy approach, is guaranteed by the following sufficient, but not necessary, orthogonality condition,[29]

$$W_p^\dagger W_q = \frac{1}{\pi}\delta_{p,q}. \tag{26}$$

This is usually the only constraint imposed on the coupling matrix describing a conventional chaotic cavity coupled to free propagation leads. In the chiral case, we find compatibility between the chiral constraint in the Hamiltonian, $\Sigma_z \mathcal{H} \Sigma_z = -\mathcal{H}$, and in the scattering matrix, $S(E) = S^\dagger(-E)$, only if the coupling matrices satisfy the extra constraint,

$$\Sigma_z W_j = W_j, \quad j = 1,2. \tag{27}$$

In the following sections, we shall present the results for chiral Hamiltonians with $\beta=1$, 2, and 4 and coupling matrices satisfying both Eqs. (26) and (27). The conductance and shot-noise power are obtained from the transmission matrix [Eq. (22)] by using Eqs. (7) and (8). Such procedure can be quite demanding since we must invert a $M \times M$ complex matrix for each realization, with in principle $M \gg 1$. We observed that, in the limit of few open channels, good results can be obtained with relatively small values for M since we generate a large number of realizations. The numerical data in the next section were obtained from 30×30 matrices $\mathcal{H}$ and 30 000 realizations. The number of zero modes is fixed by $N_z = \min(N_1, N_2)$.

III. PHYSICAL RESULTS

In this section, we restrict our attention to some particular cases of physical interest. We begin by analyzing the extreme quantum limit of a few number of open channels. We analytically obtain the full distribution of conductance for the cases $N_1 = N_2 = 1$ and $N_1 = N_2 = 2$. We also study the intermediate regime $N_1 = 1$ and $N_2 = 1 + m$, in which we can investigate the effects on the conductance distribution of opening the scattering channels by increasing m. All results are supported by extensive numerical simulations of the Mahaux–Weidemüller formula. Finally, we derive the average conductance for arbitrary N_1 and N_2.

A. Extreme quantum regime ($N_1 = 1 = N_2$)

The study of statistical properties in the extreme quantum limit is very important since it reveals information about quantum transport in a nonperturbative regime that is experimentally accessible.[30]

For the single-mode case ($N_1 = 1 = N_2$), the eigenvalue distribution [Eq. (15)] simplifies to

$$P(\phi) = \frac{2\Gamma(\beta/2 + 1/2)}{\sqrt{\pi}\Gamma(\beta/2)} \sin^{\beta-1}(2\phi), \tag{28}$$

from which we obtain the moments of the conductance and shot-noise power,

$$\langle g^n \rangle = \prod_{j=0}^{n-1} \frac{(\beta + 2j)}{(\beta + 2j + 1)}, \tag{29}$$

$$\langle p^n \rangle = \prod_{j=0}^{n-1} \frac{(2j+1)(\beta + 2j)}{(\beta + 4j + 1)(\beta + 4j + 3)}, \quad n = 1,2, \ldots . \tag{30}$$

The full distributions of these observables are obtained by a simple change of variables in Eq. (28). The conductance distribution, for instance, is obtained from the relation $g = \sin^2 2\phi$, while the distribution of shot-noise power is obtained from $p = \sin^2 2\phi \cos^2 2\phi$, resulting, respectively, in

$$P(g) = \frac{\Gamma(\beta/2 + 1/2)}{\sqrt{\pi}\Gamma(\beta/2)} \frac{g^{\beta/2-1}}{\sqrt{1-g}}, \tag{31}$$

$$W(p) = \frac{\Gamma(\beta/2 + 1/2)}{\Gamma(\beta/2)\sqrt{(1-4p)\pi}} \sum_{\sigma=\pm} \frac{\lambda_\sigma^{\beta/2-1}}{\sqrt{1-\lambda_\sigma}}, \tag{32}$$

where $\lambda_\sigma = (1 + \sigma\sqrt{1-4p})/2$. For conventional dots, the corresponding conductance and shot-noise power distributions were obtained in Refs. 31 and 32, respectively. Their analytical expressions are presented below,

$$P(g) = \frac{\beta}{2} g^{\beta/2-1}, \tag{33}$$

$$W(p) = \frac{\beta}{2\sqrt{(1-4p)}} \sum_{\sigma=\pm} \lambda_\sigma^{\beta/2-1}, \tag{34}$$

which are significantly different from their chiral counterparts. In Fig. 1, we compare the distributions of conductance and shot-noise power for all Wigner–Dyson and chiral classes ($\beta = 1,2,4$).

The chiral symmetry, thus, has a dramatic effect on the distribution of transport observables in the extreme quantum limit. Figure 1 also exhibits numerical results obtained form the Mahaux–Weidenmüller formula. The agreement between analytical and numerical results is a striking confirmation of the correctness of the maximum-entropy hypothesis in this problem.

From the general shape of the distributions, we also conclude that the presence of chiral symmetry induces an opening of propagation channels, which, in turn, enhances the regularity of charge transmission events by suppressing the corresponding shot noise.

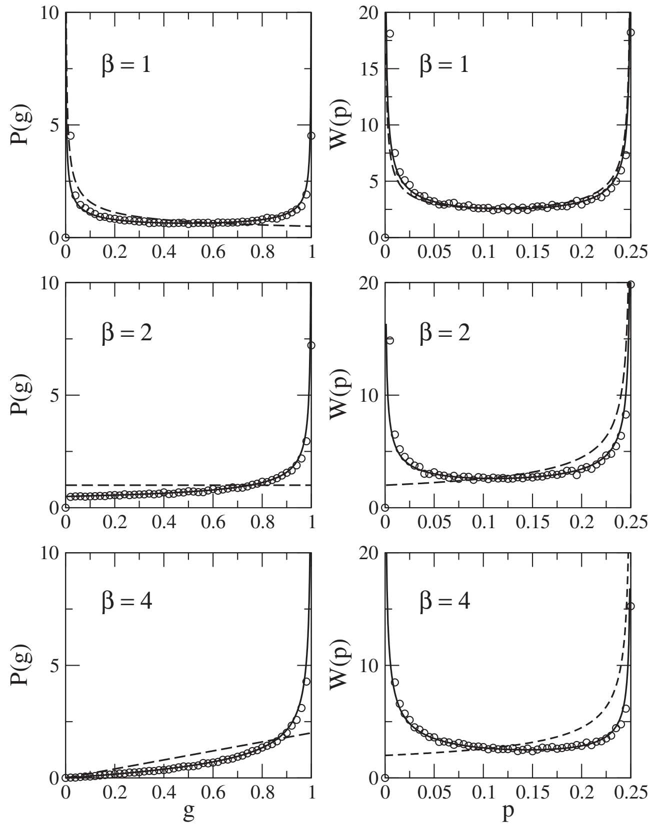

FIG. 1. Conductance (left) and shot-noise power (right) distributions for $N_1=N_2=1$ and $\beta=1,2,4$. The chiral classes are represented by the solid lines, whereas those of the Wigner–Dyson case are the dotted ones. The open circles are numerical data for the chiral class.

B. Symmetric contacts with two open channels ($N_1=2=N_2$)

This case is slightly more complex than the previous one since we have another factor describing correlations between the transmission eigenvalues. The joint distribution is given by

$$P(\phi_1,\phi_2) = C_\beta|\sin(\phi_1+\phi_2)\sin(\phi_1-\phi_2)|^\beta \times\sin^{\beta-1}(2\phi_1)\sin^{\beta-1}(2\phi_2), \tag{35}$$

where the normalization constant assumes the values $C_1=1$, $C_2=6$, and $C_4=175/2$. Since we have two open channels, the conductance and shot-noise power can be written as

$$g = \sin^2(2\phi_1)+\sin^2(2\phi_2), \tag{36}$$

$$p = \sin^2(2\phi_1)\cos^2(2\phi_1)+\sin^2(2\phi_2)\cos^2(2\phi_2), \tag{37}$$

whose moments can be numerically obtained from Eq. (35). In particular, for the first moment, we found the exact results, $\langle g\rangle_1=8/9$, $\langle g\rangle_2=16/15$, $\langle g\rangle_4=32/27$, $\langle p\rangle_1=56/225$, $\langle p\rangle_2=32/105$, and $\langle p\rangle_4=736/2079$, where the subscript indicates the values of β.

The full conductance distribution can be obtained by the following ensemble average:

$$P_\beta(g) = \langle\delta(g-\sin^2 2\phi_1-\sin^2 2\phi_2)\rangle, \tag{38}$$

where $\langle\cdots\rangle$ is a shorthand for $\int_0^{\pi/2}\int_0^{\pi/2}\ldots P(\phi_1,\phi_2)d\phi_1 d\phi_2$. Performing the integrals as in Appendix B of Ref. 21, we obtain for $\beta=1$ the following distribution:

$$P_1(g) = \begin{cases} \frac{1}{2}[K(g)-F(\pi/4,g)], & 0\leqslant g<1 \\ \dfrac{1}{2\sqrt{g}}[K(1/g)-F(\arcsin(\sqrt{g/2}),1/g)], & 1<g\leqslant 2, \end{cases} \tag{39}$$

where $F(\varphi,m)=\int_0^\varphi d\theta(1-m\sin^2\theta)^{-1/2}$ and $K(m)=F(\pi/2,m)$ are the incomplete and complete elliptic integrals, respectively. The distributions in the unitary and symplectic cases are given, respectively, by

$$P_2(g) = \begin{cases} \frac{3}{4}(2-g)\arcsin\left(\dfrac{g}{2-g}\right), & 0\leqslant g\leqslant 1 \\ \dfrac{3\pi}{8}(2-g), & 1\leqslant g\leqslant 2 \end{cases} \tag{40}$$

and

$$P_4(g) = \begin{cases} \frac{175}{2048}\left[2g\sqrt{1-g}(20-20g+7g^2)+(g-2)(40-60g+6g^2+7g^3)\arcsin\left(\dfrac{g}{2-g}\right)\right], & 0\leqslant g\leqslant 1 \\ \dfrac{175\pi}{4096}(7g^2+20g-20)(g-2)^2, & 1\leqslant g\leqslant 2. \end{cases} \tag{41}$$

As in the previous section, we compare the chiral conductance distributions with the Wigner–Dyson ones. For a conventional dot, such distributions were obtained in Ref. 21 for $\beta=1$ and $\beta=2$. Nevertheless, to our knowledge, the corresponding distribution for $\beta=4$ has not yet been reported. We give below the complete list,

$$P_1(g) = \begin{cases} \frac{3}{2}g, & 0\leqslant g\leqslant 1 \\ \frac{3}{2}(g-2\sqrt{g-1}), & 1\leqslant g\leqslant 2, \end{cases} \tag{42}$$

$$P_2(g) = 2(1-|1-g|)^3, \tag{43}$$

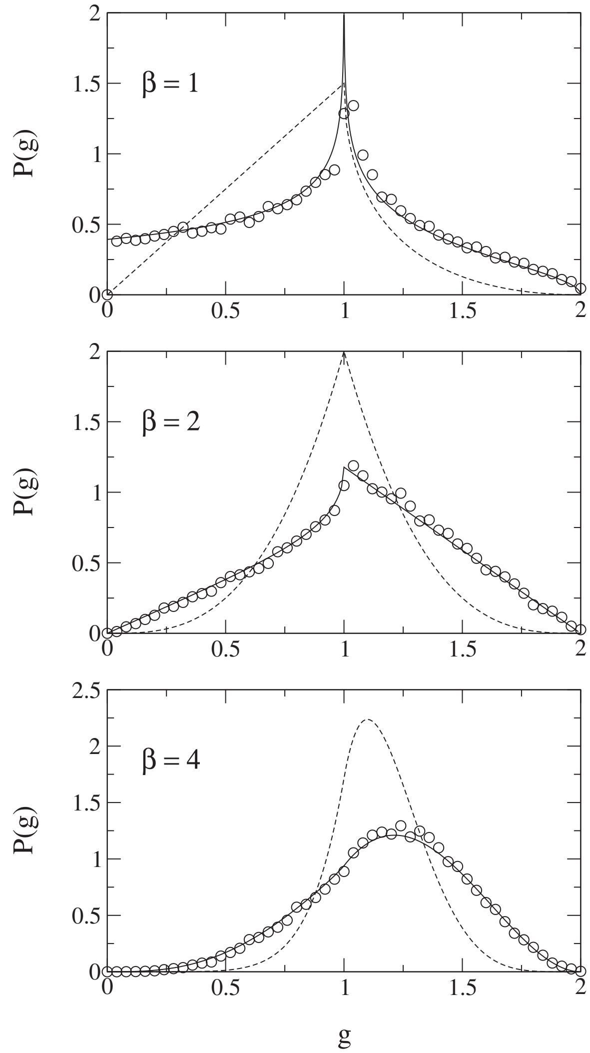

FIG. 2. Conductance distribution of a chiral quantum dot with $N_1=2=N_2$ for the three classes, $\beta=1,2,4$. The analytical result (solid line) and numerical (circles) data show an excellent agreement. The corresponding result for the Wigner–Dyson classes are plotted in dashed line.

$$P_4(g) = \begin{cases} \frac{12}{7} g^7, & 0 \leqslant g \leqslant 1 \\ \frac{12}{7}(2-g)^5(g^2+10g-10), & 1 \leqslant g \leqslant 2. \end{cases} \quad (44)$$

All distributions, chiral and Wigner–Dyson, are plotted in Fig. 2. We observe for the chiral class an excellent agreement between analytical and numerical results.

C. Asymmetric contacts ($N_1=1, N_2=1+m$)

The simplest instance of asymmetric contacts corresponds to a system with only one mode in guide 1, $N_1=1$, and an arbitrary number of modes in guide 2, $N_2=1+m$. In this case, the transmission eigenvalue distribution reads

$$P(\phi) = \frac{2^{2-\beta}\Gamma(\beta+\beta m/2)}{\Gamma(\beta/2)\Gamma(\beta/2+\beta m/2)} \sin^{\beta-1} 2\phi \sin^{\beta m} \phi. \quad (45)$$

Such expression allows for the calculation of all moments of the conductance. We find

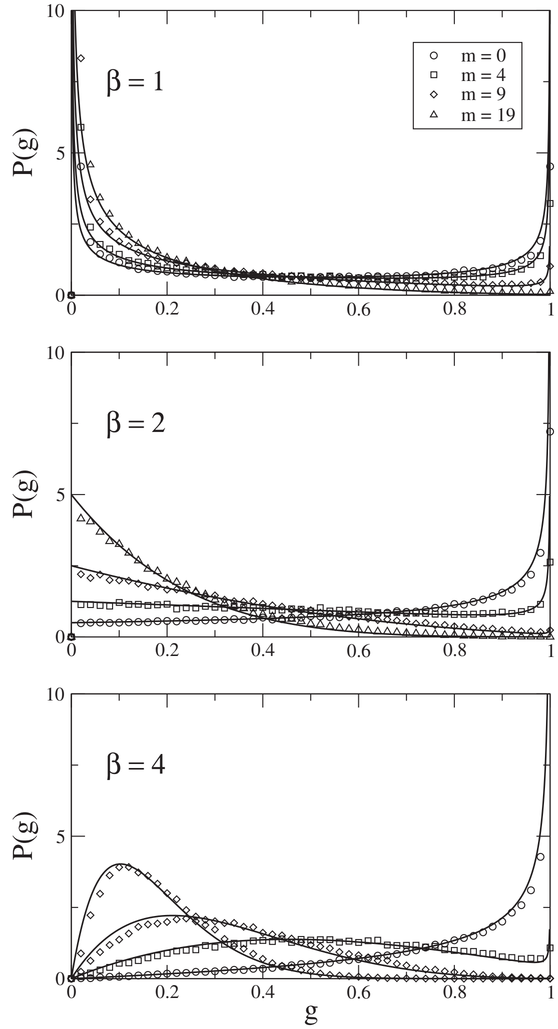

FIG. 3. Numerical (symbols) and analytical (solid lines) results for the conductance distribution of the asymmetric chiral quantum dot with $N_1=1$ and $N_2=1+m$. The graphs show the three chiral classes ($\beta=1,2,4$) for the particular values $m=0,4,9,19$.

$$\langle g^n \rangle = 2^{2n} \frac{\Gamma(n+\beta/2)\Gamma(n+\beta/2+\beta m/2)\Gamma(\beta+\beta m/2)}{\Gamma(\beta/2)\Gamma(\beta/2+\beta m/2)\Gamma(2n+\beta+\beta m/2)}. \quad (46)$$

It is also possible to obtain the full distribution of conductance,

$$P(g) = \frac{2^{-\beta(1+m/2)}\Gamma(\beta+\beta m/2)}{\Gamma(\beta/2)\Gamma(\beta/2+\beta m/2)} \times \frac{(1-\sqrt{1-g})^{\beta m/2} + (1+\sqrt{1-g})^{\beta m/2}}{g^{1-\beta/2}\sqrt{1-g}}. \quad (47)$$

Note that, in the particular case of symmetric contacts, $m=0$, Eqs. (45)–(47) agree with Eqs. (28), (29), and (31). In Fig. 3, we show the analytical and numerical results for the conductance distribution with $m=0,4,9,19$.

We observe that the graphs show a tendency of the distributions to be concentrated on small conductances as the number of channels in one of the leads is increased.

D. Average conductance for general N_1 and N_2

For an arbitrary number of open channels, it is convenient to perform the following change of variables in Eq. (15), $x_i=\cos(2\phi_i)$. The probability distribution in the variables acquires the simple form,

$$P(\{x\}) = C_N \prod_{i<j} |x_i - x_j|^\beta \prod_i w(x_i), \quad (48)$$

where $w(x)=(1-x^2)^{(\beta-2)/2}(1-x)^{m\beta/2}$ and $-1 \leqslant x_i \leqslant 1$. This expression is known in random-matrix theory as the Jacobi ensemble.[20] In this parametrization, the conductance is given by

$$g = \sum_{i=1}^{N} (1 - x_i^2). \quad (49)$$

The average conductance then reads

$$\langle g \rangle = N - \langle X_2 \rangle, \quad (50)$$

where

$$\langle X_2 \rangle = \int d^N x \left(\sum_i x_i^2 \right) P(\{x\}). \quad (51)$$

The integral in Eq. (51) can be calculated by using the Fokker–Planck methods developed for the Brownian motion ensembles in Ref. 33. In such approach, the levels, represented by the variables x_i, execute an artificial Brownian motion that has a stationary solution P_{st} given by the joint distribution of the Jacobi ensemble [Eq. (48)]. According to the general criteria put forward in Ref. 33, the joint probability distribution of the levels x_i evolves according to the Fokker-Planck equation,

$$\frac{\partial P}{\partial t} = \sum_{i=1}^{N} \frac{\partial}{\partial x_i} s(x_i) P_{st} \frac{\partial}{\partial x_i} \frac{P}{P_{st}}, \quad (52)$$

where $s(x)=1-x^2$. It proved useful to introduce the auxiliary function,

$$r(x) = \frac{1}{w(x)} \frac{d}{dx}[w(x)s(x)] = -\frac{\beta(m+2)}{2} x - \frac{\beta m}{2}. \quad (53)$$

The value of $\langle X_2 \rangle$ was obtained in Appendix D of Ref. 33 for the following choice $s(x)=s_2x^2+s_1x+s_0$ and $r(x)=r_1x+r_0$. In our particular case, we may set $s_0=1$, $s_1=0$, $s_2=-1$, $r_0=-\beta m/2$, and $r_1=-\beta(m+2)/2$, which yield

$$\langle g \rangle = \frac{4\beta N^2 (N+m)^2}{(2N+m-1)(2N+m)[\beta(2N+m)+2]}. \quad (54)$$

Since $N+m=N_2$ and $2N+m=N_1+N_2$, we can write

$$\langle g \rangle = \frac{4\beta (N_1 N_2)^2}{(N_1+N_2-1)(N_1+N_2)[\beta(N_1+N_2)+2]}. \quad (55)$$

This result reduces, in the particular case $N_1=1=N_2$, to

$$\langle g \rangle = \frac{\beta}{1+\beta}, \quad (56)$$

which agrees with Eq. (29) for $n=1$. For $N_1=2=N_2$, it simplifies to

$$\langle g \rangle = \frac{8\beta}{3+6\beta}, \quad (57)$$

in agreement with the results of Sec. III B. Finally, for $N_1=1$ and $N_2=1+m$, Eq. (55) reduces to

$$\langle g \rangle = \frac{4(m+1)\beta}{(m+2)[2+\beta(2+m)]}, \quad (58)$$

which agrees with Eq. (46) for $n=1$. It also reduces to the result of Ref. 18 in the particular case of $N_1=N_2=N$. For a Wigner–Dyson quantum dot, the average conductance is given by[3]

$$\langle g \rangle_{WD} = \frac{\beta N_1 N_2}{\beta(N_1+N_2)+2-\beta}. \quad (59)$$

This expression, in the semiclassical regime $N_1, N_2 \gg 1$, has the following expansion:

$$\langle g \rangle_{WD} = \frac{N_1 N_2}{N_1+N_2} + \frac{\beta-2}{\beta} \frac{N_1 N_2}{(N_1+N_2)^2} + \ldots . \quad (60)$$

The dominant term is the classical effective conductance obtained from a series composition. The term of order 1 is a quantum correction with a sign consistent with weak localization for $\beta=1$ and with weak antilocalization for $\beta=4$. The semiclassical expansion for the chiral case reads

$$\langle g \rangle_{ch} = \frac{4(N_1 N_2)^2}{(N_1+N_2)^3} + \frac{\beta-2}{\beta} \frac{4(N_1 N_2)^2}{(N_1+N_2)^4} + \ldots . \quad (61)$$

Note that the leading term does not coincide with the Wigner–Dyson one. This unexpected result is another nontrivial effect of the chiral symmetry and may have an interesting impact in the development of a chiral version of circuit theory.[34,35] Such effect does not appear if both N_1 and N_2 are of the same order, i.e., if m is small compared to N. This can be seen by expanding the leading term according to

$$\frac{4(N_1 N_2)^2}{(N_1+N_2)^3} = \frac{N_1 N_2}{(N_1+N_2)} \left(1 - \frac{m^2}{4N^2} + \mathcal{O}(m^3/N^3) \right). \quad (62)$$

In particular, in the symmetric case ($N_1=N_2$), the chiral symmetry does not affect the leading term.[18]

IV. CONCLUSION

In this paper, we have presented two independent random matrix approaches to the study of universal transport properties of a quantum dot with chiral symmetry, coupled to a chiral symmetric environment by two asymmetric ideal point contacts. We constructed the S-matrix ensemble by calculating the Haar measure of the appropriate symmetry group, from which we obtained the joint distribution of transmission eigenvalues. It was possible to analytically obtain all moments and the full distribution of the conductance in some interesting cases. We also obtained, from a Fokker–Planck approach, the average conductance for arbitrary values of open propagating channels in each lead. We observed that the presence of chiral symmetry affects all terms in the semiclassical expansion including the dominant one. This nontrivial effect vanishes if the asymmetry parameter m is sufficiently small or if the environment breaks chiral symmetry. We also modeled the closed quantum dot by a chiral random Hamiltonian and numerically obtained the S-matrix by means of the Mahaux–Weidenmüller formula. We showed that both approaches agree if the matrix describing the coupling between resonance states in the dot and scattering states in the leads satisfies an additional constraint. The agreement between analytical and numerical results confirms the correctness of the maximum-entropy hypothesis.

ACKNOWLEDGMENTS

This work was partially supported by CNPq and FACEPE (Brazilian Agencies).

APPENDIX: INVARIANT MEASURE

In this section, we derive the invariant measures for the S-matrix ensembles. The standard procedure[21] is based on the following definition of the differential arc element:

$$ds^2 = \mathrm{Tr}[dS^\dagger dS]. \tag{A1}$$

From differential geometry, the arc element allows from the identification of the metric tensor through the formula

$$ds^2 = \sum_{\mu,\nu} g_{\mu\nu}\delta x_\mu \delta x_\nu, \tag{A2}$$

which implies the following invariant volume element:

$$dV = |\det g|^{1/2}\prod_\mu \delta x_\mu. \tag{A3}$$

In the next subsections, we follow this procedure to construct the invariant measures of all chiral symmetry classes.

1. Orthogonal ensemble

For the orthogonal ensemble, the S-matrix satisfies $SS^\dagger = 1$ and $S=S^\dagger=S^T$ and can be written in the polar representation as

$$S = VRV^T = \begin{pmatrix} v & 0 \\ 0 & u \end{pmatrix}\begin{pmatrix} -A & B \\ B^T & C \end{pmatrix}\begin{pmatrix} v^T & 0 \\ 0 & u^T \end{pmatrix}, \tag{A4}$$

where v and u are real orthogonal matrices of order N_1 and N_2, respectively, and A and C are diagonal matrices also of order N_1 and N_2 defined by

$$A = [\sqrt{\rho}]_{N_1\times N_1}, \quad C = \begin{pmatrix} \mathbb{1}_m & 0_{m\times N_1} \\ 0_{N_1\times m} & A \end{pmatrix}_{N_2\times N_2}, \tag{A5}$$

and B is a rectangular matrix given by

$$B = [0_{N_1\times m}, [\sqrt{\tau}]_{N_1\times N_1}]_{N_1\times N_2}, \tag{A6}$$

where, for the sake of simplicity, we defined $\rho = 1-\tau$. Such matrices can be explicitly written as

$$A = \begin{pmatrix} \sqrt{\rho_1} & 0 & \cdots & 0 \\ 0 & \sqrt{\rho_2} & \cdots & 0 \\ \vdots & \vdots & \ddots & \vdots \\ 0 & 0 & \cdots & \sqrt{\rho_{N_1}} \end{pmatrix}_{N_1\times N_1}, \tag{A7}$$

$$C = \begin{pmatrix} 1 & \cdots & 0 & 0 & \cdots & 0 \\ \vdots & \ddots & \vdots & \vdots & \ddots & \vdots \\ 0 & \cdots & 1 & 0 & \cdots & 0 \\ 0 & \cdots & 0 & \sqrt{\rho_1} & \cdots & 0 \\ \vdots & \ddots & \vdots & \vdots & \ddots & \vdots \\ 0 & \cdots & 0 & 0 & \cdots & \sqrt{\rho_{N_1}} \end{pmatrix}_{N_2\times N_2}, \tag{A8}$$

and

$$B = \begin{pmatrix} 0 & \cdots & 0 & \sqrt{\tau_1} & 0 & \cdots & 0 \\ 0 & \cdots & 0 & 0 & \sqrt{\tau_2} & \cdots & 0 \\ \vdots & \ddots & \vdots & \vdots & \vdots & \ddots & \vdots \\ 0 & \cdots & 0 & 0 & 0 & 0 & \sqrt{\tau_{N_1}} \end{pmatrix}_{N_1\times N_2}. \tag{A9}$$

Representation (A4) uses $N_1 + N_1(N_1-1)/2 + N_2(N_2-1)/2$ free real parameters, which are more than the necessary number, N_1N_2, resulting from the symmetry restrictions. On the other hand, parametrization (A4) is not unique, but it remains invariant under the transformation $V \to V\mathbb{G}$, where

$$\mathbb{G} = \begin{pmatrix} \mathbb{1}_{N_1} & \mathbf{0}_{N_1\times N_2} \\ \mathbf{0}_{N_2\times N1} & G_{N_2\times N_2} \end{pmatrix}, \tag{A10}$$

in which

$$G = \begin{pmatrix} \gamma_{m\times m} & \mathbf{0}_{m\times N_1} \\ \mathbf{0}_{N_1\times m} & \mathbb{1}_{N_1} \end{pmatrix}, \tag{A11}$$

and γ is a orthogonal matrix, $\gamma\gamma^T = 1_m$. The $m(m-1)/2$ degrees of freedom associated with the orthogonal matrix γ can be used to eliminate the redundancy, and we end up with a total of N_1N_2 degrees of freedom.

Differentiating S, we obtain

$$dS = V[(\delta V)R + dR + R(\delta V)^T]V^T, \tag{A12}$$

where we introduced the antisymmetric matrix $\delta V = V^T dV$. The arc element becomes

$$\begin{aligned} ds^2 = \mathrm{Tr}[&(dR)^2 + dR(\delta V)R + (\delta V)RdR + (dR)R(\delta V)^T \\ &+ (\delta V)R^2(\delta V)^T + R(\delta V)^T dR + (\delta V)R(\delta V)R \\ &+ R(\delta V)^T(\delta V)R + R(\delta V)^T R(\delta V)^T]. \end{aligned} \tag{A13}$$

From the cyclic property of the trace and the identities $(\delta V)^T = -\delta V$ and $RdR = -dRR$, we can show that $\mathrm{Tr}[(\delta V)RdR] = \mathrm{Tr}[dR(\delta V)R] = \mathrm{Tr}[(dR)R(\delta V)^T]$

$=\mathrm{Tr}[R(\delta V)^T dR]=0$. Therefore, arc element (A13) simplifies to

$$ds^2 = \mathrm{Tr}[(dR)^2 + 2(\delta V)^T \delta V + 2(\delta V)R(\delta V)R]. \quad (A14)$$

From the block structure of the matrices R, B, and V, we have

$$\mathrm{Tr}[(\delta V)^T \delta V] = \mathrm{Tr}[(\delta v)^T(\delta v)] + \mathrm{Tr}[(\delta u)^T(\delta u)],$$

$$\mathrm{Tr}[(\delta V)R(\delta V)R] = \mathrm{Tr}[(\delta v)A(\delta v)A] + 2\mathrm{Tr}[(\delta v)B(\delta u)B^T] + \mathrm{Tr}[(\delta u)C(\delta u)C].$$

By evaluating the matrix products and recalling that δv and δu are antisymmetric matrices, we find

$$\mathrm{Tr}[(\delta v)^T \delta v] = 2\sum_{a<b=1}^{N_1}[(\delta v)_{ab}]^2,$$

$$\mathrm{Tr}[(\delta u)^T \delta u] = 2\sum_{a<b=1}^{m}[(\delta u)_{ab}]^2 + 2\sum_{a<b=m+1}^{N_2}[(\delta u)_{ab}]^2 + 2\sum_{a=1}^{m}\sum_{b=m+1}^{N_2}[(\delta u)_{ab}]^2,$$

$$\mathrm{Tr}[(dR)^2] = \frac{1}{2}\sum_{a=1}^{N_1}\frac{(d\tau_a)^2}{\tau_a\rho_a},$$

$$\mathrm{Tr}[(\delta v)A(\delta v)A] = -2\sum_{a<b=1}^{N_1}\sqrt{\rho_a\rho_b}[(\delta v)_{ab}]^2,$$

$$\mathrm{Tr}[(\delta v)B(\delta u)B^T] = -2\sum_{a<b=1}^{N_1}\sqrt{\tau_a\tau_b}(\delta v)_{ab}(\delta u)_{a+m,b+m},$$

$$\mathrm{Tr}[\delta u C \delta u C] = -2\sum_{a<b=1}^{m}[(\delta u)_{ab}]^2 - 2\sum_{a<b=m+1}^{N_2}\sqrt{\rho_{a-m}\rho_{b-m}}[(\delta u)_{ab}]^2 - 2\sum_{a=1}^{m}\sum_{b=m+1}^{N_2}\sqrt{\rho_{b-m}}[(\delta u)_{ab}]^2.$$

By substituting these expressions in Eq. (A14) and rearranging some terms, we obtain the final expression for the arc element,

$$ds^2 = 4\sum_{a<b=1}^{N_1}[(1-\sqrt{\rho_a\rho_b})([(\delta v)_{ab}]^2 + [(\delta u)_{a+m,b+m}]^2) - 2\sqrt{\tau_a\tau_b}(\delta v)_{ab}(\delta u)_{a+m,b+m}] + 4\sum_{a=1}^{m}\sum_{b=1}^{N_1}(1-\sqrt{\rho_b}) \times[(\delta u)_{a,b+m}]^2 + \frac{1}{2}\sum_{a=1}^{N_1}\frac{(d\tau_a)^2}{\tau_a\rho_a}. \quad (A15)$$

In Eq. (A15), we have $d\tau_a$ $(a=1,\ldots,N_1)$, contributing with N_1 independent variations, $(\delta v)_{ab}$ and $(\delta u)_{a+m,b+m}$, $(1,\ldots,a<b,\ldots,N_1)$, contributing with $N_1(N_1-1)/2$ each, and $(\delta u)_{ab}$, with $a=1,\ldots,m$ and $b=1,\ldots,N_1$, contributing with mN_1, giving a total of

$$N_1 + 2\frac{N_1(N_1-1)}{2} + (N_2-N_1)N_1 = N_1N_2, \quad (A16)$$

which is the correct number of independent parameters.

The metric tensor has a simple structure consisting of $N_1(N_1-1)/2$ blocks with rows and columns labeled by $(\delta v)_{ab}$ and $(\delta u)_{a+m,b+m}$,

$$\begin{array}{c|cc} & (\delta v)_{ab} & (\delta u)_{a+m,b+m} \\ \hline (\delta v)_{ab} & 1-\sqrt{\rho_a\rho_b} & -\sqrt{\tau_a\tau_b} \\ (\delta u)_{a+m,b+m} & -\sqrt{\tau_a\tau_b} & 1-\sqrt{\rho_a\rho_b} \end{array}, \quad (A17)$$

one N_1-dimensional block,

$$\mathrm{diag}\left(\frac{1}{\tau_1\rho_1},\ldots,\frac{1}{\tau_{N_1}\rho_{N_1}}\right), \quad (A18)$$

related to the increments $d\tau_a$ and m N_1-dimensional blocks,

$$\mathrm{diag}(1-\sqrt{\rho_1},\ldots,1-\sqrt{\rho_{N_1}}), \quad (A19)$$

related to the differentials $(\delta u)_{a+m,b+m}$, $a=1,\ldots,m$ and $b=1,\ldots,N_1$. Therefore, the determinant of the metric tensor reads

$$\det g \propto \prod_{a<b=1}^{N_1}[(1-\sqrt{\rho_a\rho_b})^2 - \tau_a\tau_b]\prod_{a=1}^{N_1}\frac{(1-\sqrt{\rho_a})^m}{\tau_a\rho_a}. \quad (A20)$$

Thus, the invariant measure directly follows from Eq. (A3). Its radial part is related to the joint distribution of transmission eigenvalues,

$$P(\{\tau\}) \propto \prod_{a<b}|(1-\sqrt{\rho_a\rho_b})^2 - \tau_a\tau_b|^{1/2}\prod_a\frac{(1-\sqrt{\rho_a})^{m/2}}{\sqrt{\tau_a\rho_a}}. \quad (A21)$$

This expression can be simplified by introducing the angles ϕ_a through the relation $\tau_a=\sin^2 2\phi_a$. The resulting angular distribution reads

$$P(\{\phi\}) \propto \prod_{a<b}\prod_{\sigma=\pm}|\sin(\phi_a+\sigma\phi_b)|\prod_a \sin^m(\phi_a), \quad (A22)$$

which corresponds to Eq. (15) for $\beta=1$.

2. Unitary ensemble

For the unitary ensemble, the S-matrix satisfies $SS^\dagger=1$ and $S=S^\dagger$ and can be written in the same structure of Eq. (A4),

$$S = VRV^\dagger = \begin{pmatrix} v & 0 \\ 0 & u \end{pmatrix}\begin{pmatrix} -A & B \\ B^T & C \end{pmatrix}\begin{pmatrix} v^\dagger & 0 \\ 0 & u^\dagger \end{pmatrix}, \quad (A23)$$

but with v and u being unitary matrices. In this case, the number of used parameters is $N_1^2+N_2^2+N_1$, which is different from the necessary $2N_1N_2$ parameters imposed by the Hermiticity and unitarity constraints of the S-matrix. Parametrization (A23) is also not unique. It is invariant under the transformation $V \to V\mathbb{G}$, with

$$\mathbb{G} = \begin{pmatrix} d_{N_1\times N_1} & \mathbf{0}_{N_1\times N_2} \\ \mathbf{0}_{N_2\times N1} & U_{N_2\times N_2} \end{pmatrix}, \tag{A24}$$

in which

$$U = \begin{pmatrix} \gamma_{m\times m} & \mathbf{0}_{m\times N_1} \\ \mathbf{0}_{N_1\times m} & d_{N_1\times N_1} \end{pmatrix}, \tag{A25}$$

where $d = \mathrm{diag}(e^{i\theta_1}, \ldots, e^{i\theta_{N_1}})$ and γ is an unitary matrix, $\gamma\gamma^\dagger = 1_m$. The N_1 and m^2 real parameters associated with the matrices d and γ, respectively, can be used to eliminate the redundancy of parametrization (A23).

By differentiating S, introducing the anti-Hermitian matrix $\delta v = v^\dagger dv$ and $\delta u = u^\dagger du$, and following the same steps as in the previous section, we can write the arc element as

$$ds^2 = \mathrm{Tr}[(dR)^2 + 2(\delta v)^\dagger(\delta v) + 2(\delta u)^\dagger(\delta u) + 2(\delta v)A(\delta v)A + 4(\delta v)B(\delta u)B^T + 2(\delta u)C(\delta u)C]. \tag{A26}$$

The anti-Hermitian matrices (δv and δu) can be written in terms of real symmetric (δs_1 and δs_2) and antisymmetric (δa_1 and δa_2) matrices as

$$\delta v = \delta a_1 + i\delta s_1, \quad \delta u = \delta a_2 + i\delta s_2. \tag{A27}$$

By using this decomposition and evaluating the traces as in the previous section, we obtain the final expression for the differential arc element,

$$\begin{aligned} ds^2 = {} & \sum_{a=1}^{N_1}\left(2\tau_a(\delta y_a)^2 + \frac{1}{2}\frac{(d\tau_a)^2}{\tau_a\rho_a}\right) + 4\sum_{a=1}^{m}\sum_{b=1}^{N_1}(1-\sqrt{\rho_b}) \\ & \times([(\delta a_2)_{a,b+m}]^2 + [(\delta s_2)_{a,b+m}]^2) + 4\sum_{a<b=1}^{N_1}(1-\sqrt{\rho_a\rho_b}) \\ & \times([(\delta a_1)_{ab}]^2 + [(\delta s_1)_{ab}]^2 + [(\delta a_2)_{a+m,b+m}]^2 \\ & + [(\delta s_2)_{a+m,b+m}]^2) - 8\sum_{a<b=1}^{N_1}\sqrt{\tau_a\tau_b}((\delta a_1)_{ab}(\delta a_2)_{a+m,b+m} \\ & + (\delta s_1)_{ab}(\delta s_2)_{a+m,b+m}), \end{aligned} \tag{A28}$$

in which we have defined the combination

$$\delta y_a = (\delta s_1)_{aa} - (\delta s_2)_{a+m,a+m}. \tag{A29}$$

In Eq. (A28), we have $d\tau_a$ and δy_a ($a=1,\ldots,N_1$), contributing with N_1 independent variations each. The $(\delta s_1)_{ab}$, $(\delta a_1)_{ab}$, $(\delta s_2)_{a+m,b+m}$, and $(\delta a_2)_{a+m,b+m}$ for $(1,\ldots,a < b,\ldots,N_1)$ contribute with $N_1(N_1-1)/2$ each. Finally, the $(\delta a_2)_{a,b+m}$ and $(\delta s_2)_{a,b+m}$ for $a=1,\ldots,m$ and $b=1,\ldots,N_1$ contribute with mN_1 each. The number of independent real parameters is, thus,

$$2N_1 + 4\frac{N_1(N_1-1)}{2} + 2(N_2-N_1)N_1 = 2N_1N_2, \tag{A30}$$

which is the correct number of independent parameters of a unitary and Hermitian matrix with bock structure (A23).

From Eq. (A28), we can construct the metric tensor, whose determinant is given by

$$\det g \propto \prod_{a<b}[(1-\sqrt{\rho_a\rho_b})^2 - \tau_a\tau_b]^2\prod_a\frac{(1-\sqrt{\rho_a})^{2m}}{\rho_a}, \tag{A31}$$

allowing us to obtain the joint distribution of transmission eigenvalues,

$$P(\{\tau\}) \propto \prod_{a<b}|(1-\sqrt{\rho_a\rho_b})^2 - \tau_a\tau_b|\prod_a\frac{(1-\sqrt{\rho_a})^m}{\sqrt{\rho_a}}. \tag{A32}$$

By performing the change to the variables $\tau_a = \sin^2(2\phi_a)$, we obtain the distribution

$$P(\{\phi\}) \propto \prod_{a<b}\prod_{\sigma=\pm}|\sin(\phi_a + \sigma\phi_b)|^2\prod_a \sin(2\phi_a)\sin^{2m}(\phi_a), \tag{A33}$$

which is Eq. (15) for $\beta=2$.

3. Symplectic ensemble

In the symplectic case, there is an additional spin degree of freedom in each scattering state yielding a factor 2 in the order of the scattering matrix. Therefore, S is a $2(N_1+N_2)\times 2(N_1+N_2)$ matrix, which can be treated as a $(N_1+N_2)\times(N_1+N_2)$ quaternion matrix, with the same block structure. According to the symmetry constraints, the S-matrix must be unitary ($SS^\dagger=1$), self-dual ($S=\bar{S}$), and Hermitian ($S=S^\dagger$). Such matrix must have $4N_1N_2$ free parameters and can be represented as

$$S = VR\bar{V} = \begin{pmatrix} v & 0 \\ 0 & u \end{pmatrix}\begin{pmatrix} -A & B \\ B^T & C \end{pmatrix}\begin{pmatrix} \bar{v} & 0 \\ 0 & \bar{u} \end{pmatrix}, \tag{A34}$$

where v and u are unitary and self-dual quaternion matrices. This representation contains $2N_1^2+2N_2^2+2N_1+N_2$ parameters, which is again more than the necessary number. The redundant parameters are due to the fact that parametrization (A34) also is not unique, but it is invariant under the transformation

$$u \to uu_0, \quad v \to vv_0, \tag{A35}$$

where

$$v_0 = d = \mathrm{diag}(d_1, \ldots, d_{N_1}), \quad d_i \in SU(2),$$

and

$$u_0 = \begin{pmatrix} \gamma_{m\times m} & \mathbf{0}_{m\times N_1} \\ \mathbf{0}_{N_1\times m} & d_{N_1\times N_1} \end{pmatrix}, \quad \gamma\bar{\gamma} = 1_m. \tag{A36}$$

The $3N_1$ parameters of the $SU(2)$ matrices d_i and the $2m^2+m$ of the real self-dual matrix γ can be used to eliminate the redundant parameters of Eq. (A34).

By differentiating S and introducing the anti-self-dual matrices $\delta v = \bar{v}dv$ and $\delta u = \bar{u}du$, we can write the arc element as

$$ds^2 = \mathrm{Tr}[(dR)^2 + 2\overline{(\delta v)}(\delta v) + 2\overline{(\delta u)}(\delta u) + 2(\delta v)A(\delta v)A + 4(\delta v)B(\delta u)B^T + 2(\delta u)C(\delta u)C]. \tag{A37}$$

By evaluating the last traces and using the fact that an anti-self-dual matrix δv can be expanded in the quaternion basis as an antisymmetric matrix, $\delta v^{(0)}$, and tree symmetric matrices, $\delta v^{(k)}$, $k=1,2,3$, we obtain the final expression for the differential arc element,

$$ds^2 = 4\sum_{a=1}^{N_1}\left(\tau_a\sum_{k=1}^{3}(\delta y_a^{(k)})^2 + \frac{(d\tau_a)^2}{\tau_a\rho_a}\right) + 8\sum_{a=1}^{m}\sum_{b=1}^{N_1}\sum_{k=0}^{3}(1-\sqrt{\rho_b}) \times[(\delta u^{(k)})_{a,b+m}]^2 + 8\sum_{a<b=1}^{N_1}\sum_{k=0}^{3}[(1-\sqrt{\rho_a\rho_b})([(\delta v^{(k)})_{ab}]^2 + [(\delta u^{(k)})_{a+m,b+m}]^2) - 2\sqrt{\tau_a\tau_b}(\delta v^{(k)})_{ab}(\delta u^{(k)})_{a+m,b+m}], \tag{A38}$$

in which we have defined the combination

$$\delta y_a^{(k)} = (\delta v^{(k)})_{aa} - (\delta u^{(k)})_{a+m,a+m}. \tag{A39}$$

In Eq. (A38), we have $d\tau_a$ and $\delta y_a^{(k)}$, for $a=1,\ldots,N_1$ and $k=1,2,3$, contributing with N_1 independent variations each. The $(\delta v^{(k)})_{ab}$ and $(\delta u^{(k)})_{a+m,b+m}$, for $1,\ldots,a<b,\ldots,N_1$ and $k=0,1,2,3$, contribute with $N_1(N_1-1)/2$ each. Finally, the $(\delta u^{(k)})_{a,b+m}$, for $a=1,\ldots,m$, $b=1,\ldots,N_1$, and $k=0,1,2,3$ contribute with mN_1 for each value of k. The number of independent real parameters is thus

$$4N_1 + 8\frac{N_1(N_1-1)}{2} + 4(N_2-N_1)N_1 = 4N_1N_2, \tag{A40}$$

which is the correct number of independent parameters.

From Eq. (A38), we can construct the metric tensor, whose determinant is given by

$$\det g \propto \prod_{a<b=1}^{N_1}[(1-\sqrt{\rho_a\rho_b})^2 - \tau_a\tau_b]^4\prod_{a=1}^{N_1}\frac{\tau_a^2(1-\sqrt{\rho_a})^{4m}}{\rho_a}, \tag{A41}$$

allowing us to obtain the joint distribution of transmission eigenvalues,

$$P(\{\tau\}) \propto \prod_{a<b=1}^{N_1}|(1-\sqrt{\rho_a\rho_b})^2 - \tau_a\tau_b|^2\prod_{a=1}^{N_1}\frac{\tau_a(1-\sqrt{\rho_a})^{2m}}{\sqrt{\rho_a}}. \tag{A42}$$

As in the previous sections, we change the variables according to $\tau_a=\sin^2(2\phi_a)$. The distribution function reads

$$P(\{\phi\}) \propto \prod_{a<b}\prod_{\sigma=\pm}|\sin(\phi_a+\sigma\phi_b)|^4\prod_a \sin^3(2\phi_a)\sin^{4m}(\phi_a), \tag{A43}$$

which is Eq. (15) for $\beta=4$.

[1] D. K. Ferry and S. M. Goodnick, *Transport in Nanostructures* (Cambridge University Press, Cambridge, 1997).
[2] L. S. Levitov, in *Quantum Noise in Mesoscopic Systems*, edited by Yu. V. Nazarov (Kluwer, Dordrecht, 2003).
[3] C. W. J. Beenakker, Rev. Mod. Phys. **69**, 731 (1997).
[4] C. H. Lewenkopf and H. A. Weidenmüller, Ann. Phys. (N.Y.) **212**, 53 (1991).
[5] P. W. Brouwer, Phys. Rev. B **51**, 16878 (1995).
[6] Y. V. Fyodorov and H.-J. Sommers, J. Math. Phys. **38**, 1918 (1997).
[7] M. R. Zirnbauer, J. Math. Phys. **37**, 4986 (1996).
[8] S. Helgason, *Differential Geometry, Lie Groups and Symmetric Spaces* (Academic, New York, 1978).
[9] C. Mudry, P. W. Brouwer, and A. Furusaki, Phys. Rev. B **59**, 13221 (1999).
[10] C. Mudry, P. W. Brouwer, and A. Furusaki, Phys. Rev. B **62**, 8249 (2000).
[11] P. W. Brouwer, C. Mudry, B. D. Simons, and A. Altland, Phys. Rev. Lett. **81**, 862 (1998).
[12] P. W. Brouwer, C. Mudry, and A. Furusaki, Phys. Rev. Lett. **84**, 2913 (2000).
[13] P. W. Brouwer, C. Mudry, and A. Furusaki, Nucl. Phys. B **565**, 653 (2000).
[14] M. Titov, P. W. Brouwer, A. Furusaki, and C. Mudry, Phys. Rev. B **63**, 235318 (2001).
[15] A. Altland and B. D. Simons, Nucl. Phys. B **562**, 445 (1999); J. Phys. A **32**, L353 (1999).
[16] A. Altland and R. Merkt, Nucl. Phys. B **607**, 511 (2001).
[17] P. W. Brouwer, E. Racine, A. Furusaki, Y. Hatsugai, Y. Morita, and C. Mudry, Phys. Rev. B **66**, 014204 (2002).
[18] A. F. Macedo-Junior and A. M. S. Macêdo, Phys. Rev. B **66**, 041307(R) (2002).
[19] Yan V. Fyodorov and A. Ossipov, Phys. Rev. Lett. **92**, 084103 (2004).
[20] M. L. Mehta, *Random Matrices* (Academic, New York, 1991).
[21] P. A. Mello and H. U. Baranger, Waves Random Media **9**, 105 (1999).
[22] P. W. Brouwer and C. W. J. Beenakker, J. Math. Phys. **37**, 4904 (1996).
[23] M. Caselle and U. Magnea, Phys. Rep. **394**, 41 (2004).
[24] P. J. Forrester, J. Phys. A **39**, 6861 (2006).
[25] P. J. Forrester, Log-Gases and Random Matrices (http://www.ms.unimelb.edu.au/~matjpf/matpjf.html).
[26] J. J. M. Verbaarschot and T. Wetting, Annu. Rev. Nucl. Part. Sci.

50, 343 (2000).

[27] C. Mahaux and H. A. Weidenmüller, *Shell-Model Approach to Nuclear Reactions* (North-Holland, Amsterdam, 1969).

[28] A. M. S. Macêdo, Phys. Rev. B **63**, 115309 (2001).

[29] J. J. M. Verbaarschot, H. A. Weidenmüller, and M. R. Zirnbauer, Phys. Rep. **129**, 367 (1985).

[30] A. G. Huibers, S. R. Patel, C. M. Marcus, P. W. Brouwer, C. I. Duruöz, and J. S. Harris, Jr., Phys. Rev. Lett. **81**, 1917 (1998).

[31] H. U. Baranger and P. A. Mello, Phys. Rev. Lett. **73**, 142 (1994); R. A. Jalabert, J. L. Pichard, and C. W. J. Beenakker, Europhys. Lett. **27**, 255 (1994).

[32] M. H. Pedersen, S. A. van Langen, and M. Büttiker, Phys. Rev. B **57**, 1838 (1998).

[33] A. F. Macedo-Junior and A. M. S. Macêdo, Nucl. Phys. B **752**, 439 (2006).

[34] Yu. V. Nazarov, in *Handbook of Theoretical and Computational Nanotechnology*, edited by M. Rieth and W. Schommers (American Scientific, Valencia, CA, 2006).

[35] G. C. Duarte-Filho, A. F. Macedo-Junior, and A. M. S. Macêdo, Phys. Rev. B **76**, 075342 (2007).